

The electromagnetic pion form factor and its phase

Pablo Sanchez-Puertas^{a,*} and Enrique Ruiz Arriola^{a,b}

^a*Departamento de Física Atómica, Molecular y Nuclear, Universidad de Granada,
Av. de la Fuente Nueva s/n, E-18071, Granada*

^b*Instituto Carlos I de Física Teórica y Computacional, Universidad de Granada,
Av. de la Fuente Nueva s/n, E-18071, Granada*

E-mail: pablosanchez@ugr.es, earriola@ugr.es

In this work, we employ a dispersion relation that allows to recover the electromagnetic form factor of the pion from its modulus along the unitarity cut. Unlike the standard dispersive approach, this method extends in a straightforward manner above the inelastic region, allowing us to obtain the form factor's phase, as well as its real and imaginary parts. As applications, we extract the P -wave $\pi\pi$ phase shift, the octet form factor, derive bounds in the spacelike region, and offer insights into the onset of perturbative QCD.

*10th International Conference on Quarks and Nuclear Physics (QNP2024)
8-12 July, 2024
Barcelona, Spain*

*Speaker

1. Introduction

The electromagnetic form factor of the pion, $F_Q^\pi(q^2)$, is defined in terms of the matrix element

$$\langle \pi^+(p') | J_Q^\mu(0) | \pi^+(p) \rangle = F_Q^\pi(q^2)(p + p')^\mu, \quad J_Q^\mu = \sum_q Q_q \bar{q} \gamma^\mu q, \quad (1)$$

where $q = p' - p$ is the momentum transfer. Such object encodes information about the pion internal structure and QCD dynamics. As a consequence, it inherits the non-perturbative nature of QCD, and few information is available from first principles besides its normalization, $F_Q^\pi(0) = 1$, and its high-energy behavior predicted by perturbative QCD (pQCD) [1]¹

$$F_Q^\pi(-t) \rightarrow \frac{16\pi F_\pi^2 \alpha_s}{t} \left(1 + 6.58 \frac{\alpha_s}{\pi} \left[1 + 11.75 \frac{\alpha_s}{\pi} \right] \right), \quad (2)$$

yet the scale where this applies is not clear at all. This form factor plays an important role in hadronic physics at low and intermediate energies. For instance, it plays a central role in the muon (g-2) [3], where its modulus, accessible via the $e^+e^- \rightarrow \pi^+\pi^-$ reaction, determines the 70% of the full hadronic contributions. This has motivated a wealth of high-precision measurements that we will take advantage of in this work. Additional important information about the form factor is encoded in its phase, which, unlike the modulus, cannot be directly measured in experiments. Of particular relevance is the phase of the form factor below the onset of inelasticities, which, aside from isospin-breaking (IB) corrections, is linked to the P -wave phase in elastic $\pi\pi$ scattering via Watson's theorem. The latter plays a key role in dispersive approaches to low-energy hadronic physics. Furthermore, the form factor's phase beyond the inelastic threshold provides valuable insights into the onset of pQCD. In our work [2], we extract such a phase using dispersion relations (DRs) that relate the phase of the form factor to its modulus above the unitarity cut. This contrasts with standard dispersive approaches building on the phase, that are not well-tailored to deal with inelasticities. Different applications are discussed: the extraction of δ_1^1 and the octet form factor; the extrapolation to the spacelike region; the onset of pQCD.

2. Dispersion relation for the modulus: phase, real and imaginary parts

The standard dispersive approach to reconstruct a variety of form factors demands partial knowledge of the relevant phase at hand. For the case of F_Q^π this can be achieved, in the absence of zeros (see [2] for discussions on zeros), by writing down Cauchy's theorem for $\ln |F_Q^\pi(s)|$. This leads to the well-known solution that we will refer to as the phase-DR,

$$F_Q^\pi(s) = \exp \left(\frac{s}{\pi} \int_{s_{th}}^{\infty} dz \frac{\delta_Q^\pi(z)}{z(z-s)} \right) = \exp \left(\frac{s}{\pi} \int_{s_{th}}^{s_{in}} dz \frac{\delta_Q^\pi(z)}{z(z-s)} \right) \exp \left(\frac{s}{\pi} \int_{s_{in}}^{\infty} dz \frac{\delta_Q^\pi(z)}{z(z-s)} \right). \quad (3)$$

In general, δ_Q^π is unknown. However, below inelastic thresholds and up to isospin corrections that we discuss later, it can be identified with δ_1^1 , and the first integral on the right-hand side of Eq. (3), known as the Omnès function, can be evaluated. The remaining integral for the inelastic region

¹We update the NLO expression in [2] with the NNLO calculation [1], adopting $\mu_R^2 \sim t$ and an asymptotic distribution amplitudes.

is phenomenologically parametrized as a series expansion. Unfortunately, this approach cannot be applied for $s \gtrsim s_{th}$, where the phase is generally unknown and would demand a complicated coupled-channel analysis. To overcome this problem, in this work we will focus on a different dispersive approach based on Refs. [4–8]. This can be obtained, in the absence of zeros, by applying Cauchy’s theorem to $\ln |F_Q^\pi(z)|/\sqrt{s_{th}-z}$ or $\ln |F_Q^\pi(z)/F_Q^\pi(s_{th})|/(s_{th}-z)^{3/2}$, leading to [2]

$$F_Q^\pi(s) = \exp\left(\frac{s\sqrt{s_{th}-s}}{\pi} \int_{s_{th}}^{\infty} dz \frac{\ln |F_Q^\pi(z)|}{z\sqrt{z-s_{th}}(z-s)}\right), \quad (4)$$

$$F_Q^\pi(s) = F_Q^\pi(s_{th})^{1-\left(\frac{s_{th}-s}{s_{th}}\right)^{3/2}} \exp\left[-\frac{s(s_{th}-s)^{3/2}}{\pi} \int_{s_{th}}^{\infty} dz \frac{\ln |F_Q^\pi(z)/F_Q^\pi(s_{th})|}{z(z-s_{th})^{3/2}(z-s)}\right], \quad (5)$$

that we will refer to as DR1 and DR2. The relations above are remarkable: they provide a direct link among a measurable quantity, $|F_Q^\pi(s)|$ along the unitarity cut, and its value in the complex plane. Compared to the standard phase-DR, the modulus-DR opens up the possibility to unveil the inelastic region provided data for its modulus is available. In particular, the phase is given as

$$\delta(s) = -\frac{s\sqrt{s-s_{th}}}{\pi} \text{PV} \int_{s_{th}}^{\infty} dz \frac{\ln |F_Q^\pi(z)|}{z\sqrt{z-s_{th}}(z-s)}, \quad (6)$$

$$\delta(s) = -\ln F_Q^\pi(s_{th}) \left(\frac{s-s_{th}}{s_{th}}\right)^{3/2} - \frac{s(s-s_{th})^{3/2}}{\pi} \text{PV} \int_{s_{th}}^{\infty} dz \frac{\ln |F_Q^\pi(z)/F_Q^\pi(s_{th})|}{z(z-s_{th})^{3/2}(z-s)}, \quad (7)$$

that we will employ below in order to disentangle the real and imaginary parts of the form factor along the unitarity cut. Finally, an important sum rule can be derived from the DRs above:

$$\frac{s_{th}^{3/2}}{\pi \ln F_Q^\pi(s_{th})} \int_{s_{th}}^{\infty} dz \frac{\ln |F_Q^\pi(z)/F_Q^\pi(s_{th})|}{z(z-s_{th})^{3/2}} = 1, \quad (8)$$

that is key for consistency checks in our work [2].

In the following, we make use of DR2 together with $BABAR$ data [9] to extract the phase of the form factor, that can be achieved reliably up to around 2.5 GeV. Remarkably, $BABAR$ ’s data span energies from threshold up to 3 GeV, and is amongst the most precise experiments, with subpercent uncertainties close to the ρ peak. The reason to exclude other experiments are (i) the tensions with other experiments with similar precision, making impossible to combine them and (ii) the fact that it is the only precise experiment including data beyond the 1 GeV region, which is necessary to check the SR in Eq. (8) and guaranteeing consistency [2]. In order to perform the numerical integral, we interpolate the data with the help of a Gounaris-Sakurai model. Note that complex phases in the model break unitarity and analytic constraints, whereas the performed DR will restore the correct analytic properties shifting the phase appropriately. To keep track of correlations, we make use of a Monte Carlo (MC) analysis, following the method in Ref. [10] to avoid d’Agostini bias. Further, we make sure that the sum rule in Eq. (8) is fulfilled for every MC fit, that ensures consistency and is only possible with $BABAR$ ’s high-energy points. Our results for the phase, real and imaginary parts of the form factor are shown in Fig. 1, where the inner error bands represent the statistical uncertainty. The outer error band includes systematic uncertainties. These arise from the modelling below 0.6 GeV; above this energy, the model yields results similar to a linear interpolation—find

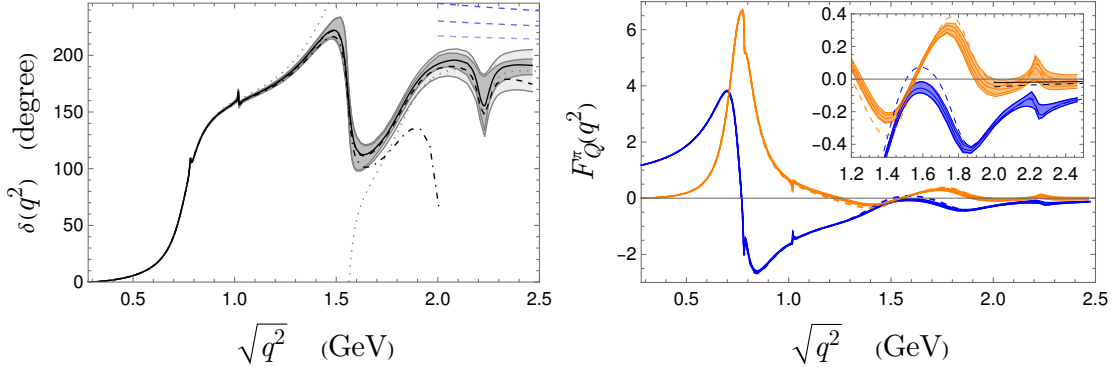


Figure 1: Left: the phase of the form factor (black line) with statistic(+systematic) inner(outer) error bands. The dot-dashed/dashed black lines are obtained for lower cutoffs in Eq. (7). The dotted gray line is the original model phase. The dashed blue lines, from light to dark, are the LO, NLO and NNLO pQCD prediction. Right: The real(imaginary) parts as blue(orange) lines with corresponding error bands similar to the left figure. The dashed blue(orange) lines are again the result from the model. The solid(dashed) black lines are the NNLO pQCD prediction for the real(imaginary) part.

details about this and the role of zeros in [2]. As it can be appreciated, the phase approaches π from above, as predicted by pQCD, yet the full result lies far from Eq. (2). A final remark is pertinent here and concerns the argument theorem in complex analysis. In our case of application, it implies that the asymptotic phase $\delta_Q^\pi \rightarrow \pi(1 + N - P)$ [2, 4], where the first term comes from pQCD and $N(P)$ stand for the number of zeros(poles) in the first Riemann sheet. For complex-conjugate poles, $\delta_Q^\pi \rightarrow \pi(1 + 2n)$, but n cannot be fixed from first principles (find comments on zeros in [2]).

3. The P -wave $\pi\pi$ phase shift and isovector/isosinglet form factors

As previously mentioned, δ_Q^π is related in the elastic region to δ_1^1 modulo isospin corrections. To show how, we decompose the electromagnetic current as $J_Q^\mu = J_3^\mu + J_8^\mu/\sqrt{3}$, with $J_a^\mu = \bar{q}\gamma^\mu \frac{\lambda^a}{2} q$ and λ^a Gell-Mann matrices, inducing the isospin decomposition $F_Q^\pi = F_3^\pi + F_8^\pi/\sqrt{3}$. Unitarity effects in the isovector form factor F_3^π first arise from $I = 1$ $\pi\pi$ interactions and, thereby, its phase identifies with δ_1^1 in the elastic region. This contrast with the octet form factor, F_8^π , that should vanish in the isospin limit and features both 2π and 3π unitarity effects at the same order in IB. These materialize in the phenomenon known as $\rho - \omega$ mixing, clearly visible in the data, that allows to perform the isospin decomposition with little model dependence [2, 11]. From the isovector one, we extract δ_1^1 in the elastic region, which is shown in Fig. 2. This is a key quantity in low-energy hadronic physics, which most precise determination has been obtained using Roy equations [12, 13], that are shown in Fig. 2. We find an excellent agreement with Ref. [13], that also uses modern input from $e^+e^- \rightarrow \pi^+\pi^-$ data. Furthermore our results are competitive in precision with Ref. [13], except at the low energy region (cf. Fig. 2 right) where systematic effects dominate.

In addition, we provide our results for the octet form factor in Fig. 3. Note that neglecting strange-quark effects, this is related to the baryonic form factor discussed in Refs. [11, 14]. As it can be appreciated, the phase approaches 2π from above—a value which is expected from the argument theorem and the real zero that follows from the null octet charge of the pion, $F_8^\pi(0) = 0$.

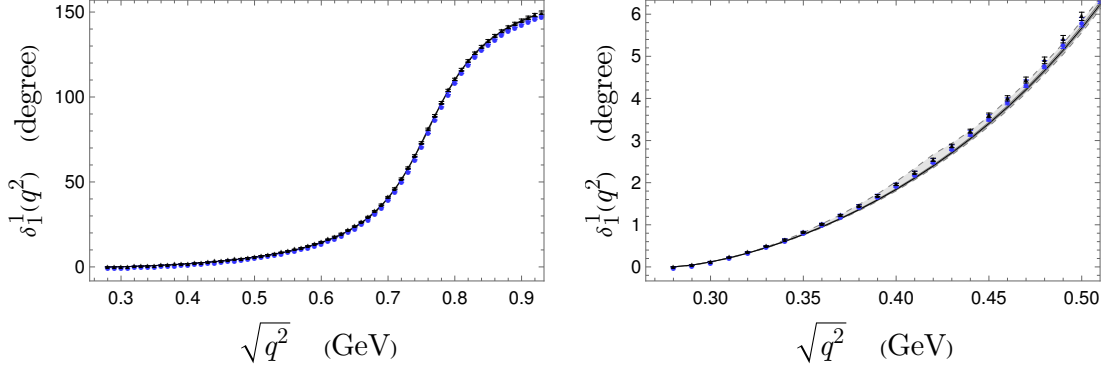


Figure 2: Left: the δ_1^1 phase shift in the full elastic region (black) compared to the result from [12] (blue bars) and [13] (black bars). Right: a detailed view of the low-energy region.

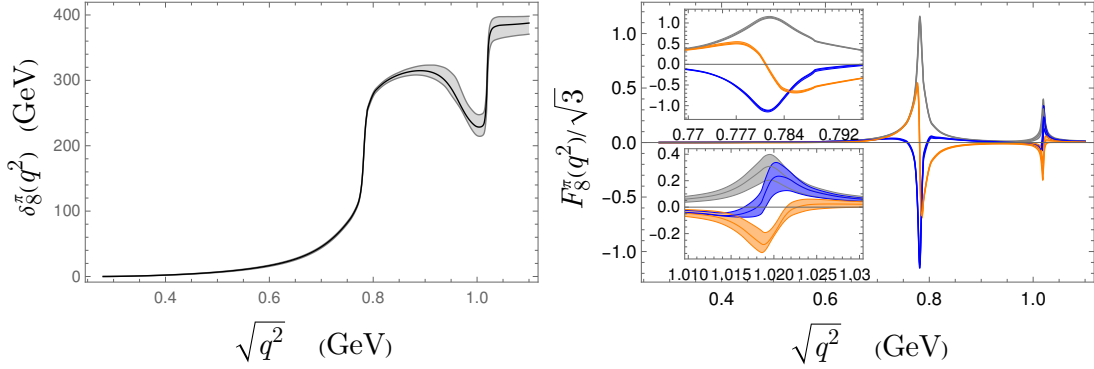


Figure 3: Left: the octet form factor phase (black) with statistical error bands (gray). Right: The real (blue), imaginary (orange) and absolute value (gray) of $F_8^\pi/\sqrt{3}$ with statistical error bands.

4. Extrapolation to the spacelike region

The DRs in Eqs. (4) and (5) can also be employed to obtain the value of the form factor in the spacelike region. Notoriously, provided the form factor lacks a steep and sustained rise at large q^2 values, Eq. (4) and Eq. (5) provide, respectively, lower and upper bounds [2]. These are illustrated in Fig. 4 (left). Interesting enough, the results resemble a VMD prediction (see also Section 5) and are far from pQCD, suggesting a late onset for the perturbative behavior. Since this is an attractive question itself, we discuss this property in the section below with the help of the sum rules.

5. Sum rules and the onset of pQCD

Using Cauchy's theorem for $F_Q^\pi(s)$, the following sum rules can be derived (see Ref. [16])

$$\frac{1}{\pi} \int_{s_0}^{\infty} ds \frac{\text{Im} F_Q^\pi(s)}{s} = 1 \quad (\text{SR1}), \quad \frac{1}{\pi} \int_{s_0}^{\infty} ds \text{Im} F_Q^\pi(s) = 0 \quad (\text{SR2}), \quad (9)$$

that follow from the normalization and pQCD asymptotics. These can be computed reliably from experiment using our result in Section 2 up to a cutoff $\Lambda_E = 2.5$ GeV without the need

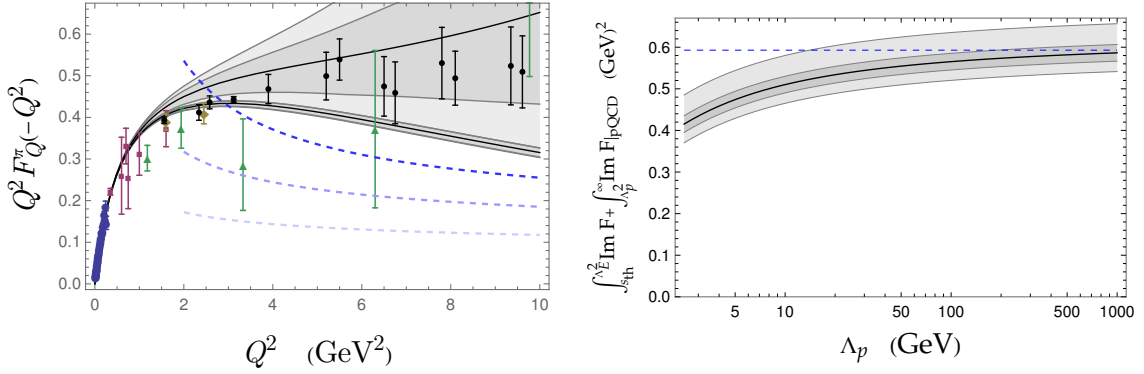


Figure 4: Left: Our upper and lower bounds for the spacelike form factor (gray bands) compared to experimental data in colors (find Refs. in [2]) and the new lattice result [15] (black bars). Right: The SR2 in Eq. (9) for different choices of the perturbative scale Λ_p .

of models. In this way, we obtain $1.01(1)({}_{-1}^{+2})$ for the SR1 (close to its nominal value), and $0.63(2)({}_{-4}^{+7})$ GeV^2 for the SR2. Interesting enough, the latter is close to the simple VMD estimate, M_ρ^2 , yet far from pQCD. One may wonder if the pQCD tail would explain such mismatch. To answer this question, we compute the pQCD contribution by analytically continuing α_s to the timelike region² and integrating from an unknown scale Λ_p (where pQCD could hypothetically be applied) up to infinity. As we illustrate in Fig. 4 (right), this is not possible even if pQCD is applied already at $\Lambda_p = \Lambda_E$. In consequence, this sum rule suggests sizeable contributions from the high-energy tail well above the pQCD prediction.

6. Conclusions and outlook

Being the lightest hadron, the pion properties are a priori amongst the simplest to be studied and measured. Yet, they continue posing challenges and attracting attention, particularly regarding its electromagnetic form factor. This is partly due to the role of the form factor in low-energy hadronic physics, where both, its modulus and phase, play an important role. Additionally, in the high-energy region, the applicability of pQCD and the transition from hadronic to quark-based descriptions remain an open and compelling questions. In this work, we have used a dispersive approach to extract both the modulus and phase, providing insight into these questions. In the future, we have plans to extend this approach to the Kaon case.

Acknowledgments

P. Sanchez Puertas would like to thank Miguel Ángel Ojeda García for local hosting and hospitality during this workshop, as well as the organizers for the nice conference and atmosphere. This work has been supported by the Spanish Ministry of Science and Innovation under Grants No. PID2020–114767GB-I00 and No. PID2023-147072NB-I00 by MICIU/AEI/10.13039/501100011033, as well as Junta de Andalucía under Grants No. POSTDOC_21_00136 and No. FQM-225.

²To do so, we take the LO result $\alpha_s = 4\pi/(\beta_0 L)$ and take $L = \ln(Q^2/\Lambda_{\text{QCD}}^2) \rightarrow \ln(s/\Lambda_{\text{QCD}}^2) - i\pi$.

References

- [1] L.-B. Chen, W. Chen, F. Feng and Y. Jia, *Next-to-Next-to-Leading-Order QCD Corrections to Pion Electromagnetic Form Factors*, *Phys. Rev. Lett.* **132** (2024) 201901 [2312.17228].
- [2] E. Ruiz Arriola and P. Sanchez-Puertas, *Phase of the electromagnetic form factor of the pion*, *Phys. Rev. D* **110** (2024) 054003 [2403.07121].
- [3] T. Aoyama et al., *The anomalous magnetic moment of the muon in the Standard Model*, *Phys. Rept.* **887** (2020) 1 [2006.04822].
- [4] T.N. Truong, R. Vinh-Mau and P. Xuan Yem, *Pion Electromagnetic Form Factor*, *Phys. Rev.* **172** (1968) 1645.
- [5] T.N. Truong and R. Vinh-Mau, *Bounds on the pion electromagnetic form-factor*, *Phys. Rev.* **177** (1969) 2494.
- [6] B.V. Geshkenbein, *Determination of the electromagnetic formfactor in the space-like region from the value of its modulus in the time - like region*, *Yad. Fiz.* **9** (1969) 1232.
- [7] C. Cronstrom, *Zeros of the pion form-factor*, *Phys. Lett. B* **49** (1974) 283.
- [8] B.V. Geshkenbein, *Pion electromagnetic form factor in the spacelike region and P phase δ_1^1 of $\pi\pi$ scattering from the value of the modulus of the form factor in the timelike region*, *Phys. Rev. D* **61** (2000) 033009 [hep-ph/9806418].
- [9] BABAR collaboration, *Precise Measurement of the $e^+e^- \rightarrow \pi^+\pi^-(\gamma)$ Cross Section with the Initial-State Radiation Method at BABAR*, *Phys. Rev. D* **86** (2012) 032013 [1205.2228].
- [10] NNPDF collaboration, *Fitting Parton Distribution Data with Multiplicative Normalization Uncertainties*, *JHEP* **05** (2010) 075 [0912.2276].
- [11] P. Sanchez-Puertas, E.R. Arriola and W. Broniowski, *Baryonic content of the pion*, *Phys. Lett. B* **822** (2021) 136680 [2103.09131].
- [12] R. Garcia-Martin, R. Kaminski, J.R. Pelaez, J. Ruiz de Elvira and F.J. Yndurain, *The Pion-pion scattering amplitude. IV: Improved analysis with once subtracted Roy-like equations up to 1100 MeV*, *Phys. Rev. D* **83** (2011) 074004 [1102.2183].
- [13] G. Colangelo, M. Hoferichter and P. Stoffer, *Two-pion contribution to hadronic vacuum polarization*, *JHEP* **02** (2019) 006 [1810.00007].
- [14] W. Broniowski, E. Ruiz Arriola and P. Sanchez-Puertas, *Baryonic form factors of the pion and kaon in a chiral quark model*, *Phys. Rev. D* **106** (2022) 036001 [2112.11049].
- [15] H.-T. Ding, X. Gao, A.D. Hanlon, S. Mukherjee, P. Petreczky, Q. Shi et al., *QCD Predictions for Meson Electromagnetic Form Factors at High Momenta: Testing Factorization in Exclusive Processes*, 2404.04412.
- [16] J.F. Donoghue and E.S. Na, *Asymptotic limits and structure of the pion form-factor*, *Phys. Rev. D* **56** (1997) 7073 [hep-ph/9611418].